ISSN 1063-7834, Physics of the Solid State, 2011, Vol. 53, No. 10, pp. 2073–2079. © Pleiades Publishing, Ltd., 2011.
Original Russian Text © M.V. Gorev, I.N. Flerov, V.S. Bondarev, M. Maglione, A. Simon 2011, published in Fizika Tverdogo Tela, 2011, Vol. 53, No. 10, pp. 1969–1974.

FERROELECTRICITY

Thermal Expansion and Permittivity of $(Ba_{1-x}Bi_{2x/3})TiO_3$ Solid Solutions

M. V. Gorev[a, b, *], I. N. Flerov[a, **], V. S. Bondarev[a, b], M. Maglione[c], and A. Simon[c]

[a] *Kirensky Institute of Physics, Siberian Branch, Russian Academy of Science, Akademgorodok, Krasnoyarsk, 660036 Russia*

* *e-mail: gorev@iph.krasn.ru*

** *e-mail: flerov@iph.krasn.ru*

[b] *Siberian Federal University, pr. Svobodnyi 79, Krasnoyarsk, 660041 Russia*

[c] *ICMCB-CNRS, Université de Bordeaux 1, Pessac, France*

Received March 17, 2011

Abstract—The strain, the thermal expansion coefficient, and the permittivity of ceramic samples of $(Ba_{1-x}Bi_{2x/3})TiO_3$ solid solutions with $x = 0$, 0.01, 0.03, and 0.05 have been studied in the temperature range 120–700 K. Based on an analysis of the results, the temperature–composition phase diagram has been refined, and the temperature dependence of the polarization has been calculated.

DOI: 10.1134/S1063783411100143

1. INTRODUCTION

In the last decades, barium titanate-based solid solutions have attracted significant interest of researchers due to a variety of their physical properties and a possibility of their applications in various technological devices. $BaTiO_3$ undergoes, with decreasing temperature, three ferroelectric transitions with alternating the phase symmetries: cubic ($Pm3m$) $\longrightarrow$ tetragonal ($P4mm$) $\longrightarrow$ orthorhombic ($C2mm$) $\longrightarrow$ rhombohedral ($R3m$) at $T_c \sim 400$ K, $T_1 \sim 290$ K, and $T_2 \sim 190$ K, respectively. Doping of $BaTiO_3$ with various impurities in positions A and/or B of the perovskite lattice is used to modify the physical properties and to shift the phase transitions to a desired temperature range [1–5]. Many of the solid solutions are characterized by the ferroelectric and relaxor properties depending on the impurity type and concentration.

Isovalent doping in positions B is usually used to change the temperature T_c and lower temperatures of the phase transitions $P4mm \longrightarrow C2mm$ (T_1) and $C2mm \longrightarrow R3m$ (T_2). For example, the doping with nonferroactive ions Zn^{4+} and Sn^{4+} leads to a linear decrease in the temperature T_c and an increase in the temperatures T_1 and T_2 [5, 6]. As the concentration of doping ion increases, many such systems demonstrate, first, wedging-out of the tetragonal and orthorhombic phases and, then, the crossover from the usual ferroelectric behavior to the relaxor behavior [6].

The heterovalent substitution of trivalent lanthanum for Ba^{2+} rapidly decreases the temperatures T_c, T_1, and T_2 [7–9]. At the lanthanum concentration of ~4–10 at %, there are relaxor phenomena that are associated with the formation of La^{3+} clusters and Ti vacancies, and the occurrence of strong random electric fields that destroy the uniform ferroelectric state [8]. In contrast to lanthanum, trivalent bismuth does not practically influence the temperature T_c up to the concentration of ~10 at %; however, at the concentration of ~2 at % Bi, anomalies of the permittivity at T_1 and T_2 coalesce into one anomaly at T_m' that appears inside the ferroelectric state, and it is characterized by a substantial frequency dispersion [10, 11].

Despite extensive studies of the materials, many aspects of phenomena proceeding in them remain unknown up to now, and they require additional studies. The thermal expansion is one of main properties that is related to many important properties of the materials, such as ferroelectric, piezoelectric, and pyroelectric properties. In addition, the order parameter in barium titanate and its derivatives is the polarization caused by displacement of ions, and the phase transitions can be detected by measuring of the thermal expansion, since the macroscopic deformation is related to the microscopic lattice deformation.

In this work, the permittivity and thermal expansion of ceramic samples of $Ba_{1-x}Bi_{2x-3}TiO_3$ with $x = 0$, 0.01, 0.03, and 0.05 were measured to refine the temperature–composition phase diagram and to determine the behavior of the root-mean-square polarization from the data on the thermal expansion.

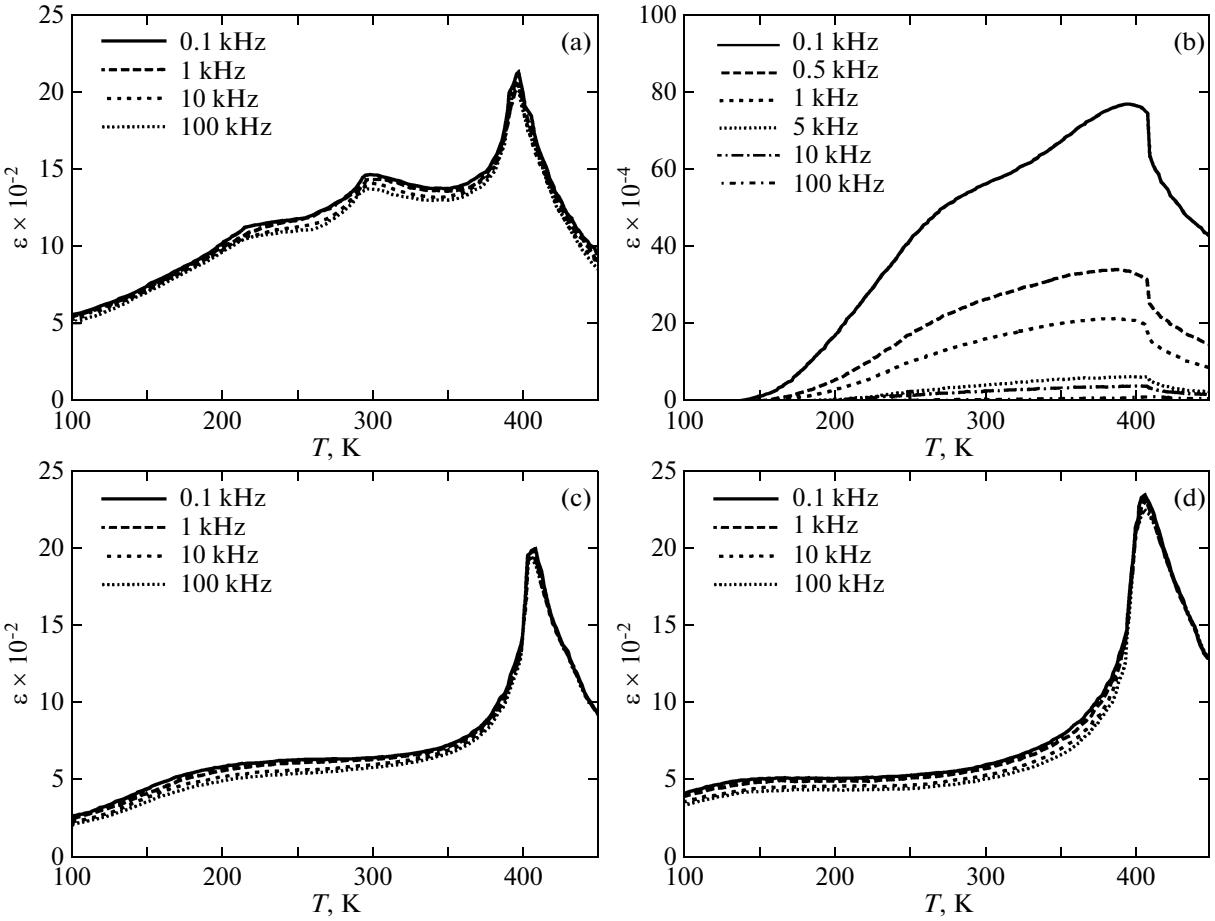

Fig. 1. Temperature dependences of the permittivity of the solid solutions $Ba_{1-x}Bi_{2x/3}TiO_3$ with $x =$ (a) 0, (b) 0.01, (c) 0.03, and (d) 0.05.

2. SYNTHESIS OF THE COMPOUNDS AND PREPARATION OF CERAMIC SAMPLES

The $Ba_{1-x}Bi_{2x/3}TiO_3$ compounds were prepared using the technique described in [11] from oxides $BaCO_2$ (Merck 99.9%), TiO_2 (Aldrich 99.99%), and Bi_2O_3 (Merck 99.9%) as a result of the solid-phase reaction $(1 - x)BaCO_3 + x/3Bi_2O_3 + TiO_2 \longrightarrow Ba_{1-x}Bi_{2x/3}TiO_3 + (1-x)CO_2$. Before heat treatment, the initial materials were carefully grinded for one hour, and, then, they were pressed into 1–5-mm-thick discs 7–8 mm in diameter at a pressure of 100 MPa. As a binder, 17% OPTARIX (Zschimmer et Schwarz) was added. After synthesizing the compounds for 2 h at 1100°C, the samples were annealed at 850°C in oxygen atmosphere for 15 h.

The X-ray diffraction studies performed at room temperature show that the samples are single-phase and that the solid solutions prepared have perovskite-type structure in the composition range $0 \le x \le 0.15$. It should be noted that the compounds are nonstoichiometric in the cation in an interoctahedral site because of the difference of the charges of Ba^{2+} and Bi^{3+}. The mass loss during heat treatments was no more than 1 wt %. The relative variations of the pellet diameter $(\Phi_{init} - \Phi_{final})/\Phi_{init}$ and the ratio of the experimental density to the theoretical density were within the limits 0f 0.05–0.18 and 0.87–0.96, respectively, and the values increase with the bismuth concentration.

3. DIELECTRIC MEASUREMENTS

The dielectric measurements were performed in the temperature range 75–450 K at frequencies of 10^2–10^5 Hz in helium atmosphere using a Wayne-Kerr 6425 analyzer. The samples were 1-mm-thick discs 7 mm in diameter with gold electrodes deposited by cathode sputtering.

The results of measuring the permittivity ε are shown in Fig. 1. It was found that, as in earlier works [10, 11], in the solid solutions with $x = -0$, 0.03, and 0.05, the position and magnitude of the maximum and also the temperature dependence of the permittivity near T_c vary insignificantly. However, the permittivity anomalies at T_1 and T_2 coalesce into one wide anom-

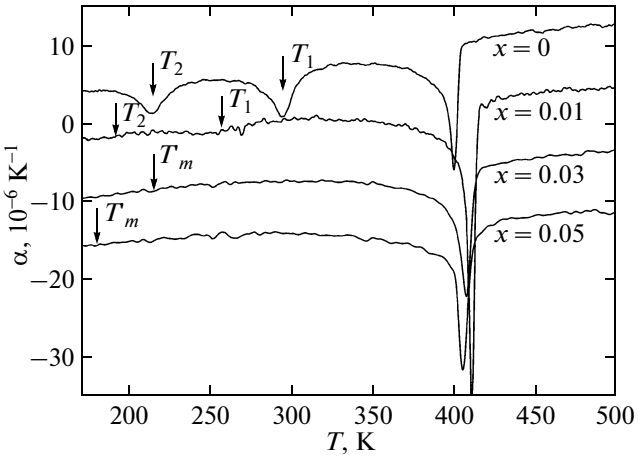

Fig. 2. Temperature dependences of the thermal expansion coefficient α of the solid solutions $Ba_{1-x}Bi_{2x/3}TiO_3$.

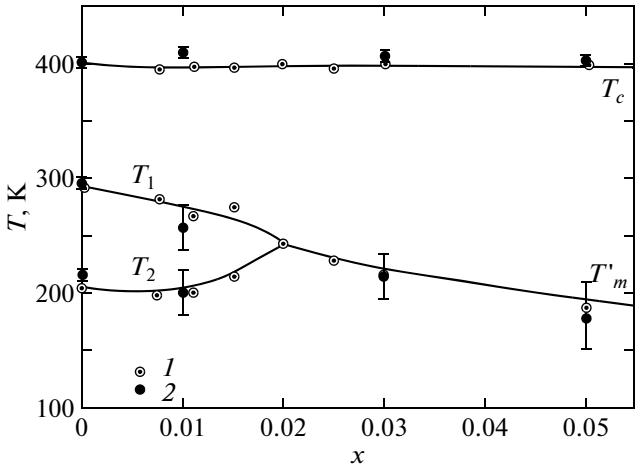

Fig. 3. Temperature–concentration phase diagram of the $Ba_{1-x}Bi_{2x/3}TiO_3$ system: (*1*) data of the dielectric studies and data taken from [11]; (*2*) results of the studies of the thermal expansion.

aly with the maximum at T'_m even in the compositions with $x \geq 0.03$.

The behavior of the solid solution with $x = 0.01$ is sharply different from other samples: its permittivity is strongly smeared over a wide temperature range covering all the phase transitions, and it is more than two orders of magnitude higher than the permittivity of other samples (Fig. 1b) at low frequency. Such a behavior at low bismuth concentration is most likely due to a nonstoichiometry of the sample, incomplete compensation of the cation charge during replacing Ba^{2+} and Bi^{3+}, and the localization of free charges at the grain boundaries. In spite of the strong dispersion of the permittivity, the anomaly temperature is independent of frequency, and it is observed at $T_c \approx 400$ K as is the case in other compositions.

4. THERMAL EXPANSION

The thermal expansion was measured on a NETZSCH DIL-402C dilatometer in the temperature range 120–700 K in the dynamic regime at a heating rate of 5 K/min on the ceramic samples with $L \approx 5$ mm. Calibration and inclusion of the thermal expansion of the measurement system was carried out using standards of fused quartz and corundum. We performed several series of the measurements for different samples of the same composition. The data of different series, as a rule, agree within the limits of the experimental error (±3%), and, because of this, the date were processed simultaneously.

The results of measuring the thermal expansion $\alpha(T)$ of the ceramic sample of pure $BaTiO_3$ and solid solutions $Ba_{1-x}Bi_{2x/3}TiO_3$ are depicted in Fig. 2 (for clarity, the curves are shifted in the plot relative to each other by -5×10^{-6} K^{-1}). The anomalies of $\alpha(T)$ in $BaTiO_3$ related to the phase transitions ($Pm3m$) ⟶ ($P4mm$) ⟶ ($C2mm$) ⟶ ($R3m$) were found at the temperatures $T_c = 400.1$ K, $T_1 = 295.5$ K, and $T_2 = 215.1$ K. The thermal expansion coefficients measured well agree with the data from [12, 13], in particular, at temperatures higher the transition temperature between the cubic and tetragonal phases.

In solid solutions $Ba_{1-x}Bi_{2x/3}TiO_3$, the anomaly of $\alpha(T)$ related to the transition from the cubic phase remains very sharp, and its magnitude is slightly dependent on the bismuth concentration. The exception is, as is the case with the dielectric measurements, the compound with $x = 0.01$ in which the anomaly of the thermal expansion coefficient is as large as twice. The low-temperature anomalies of the thermal expansion are quite quickly smeared as the bismuth concentration increases, and they are practically undetectable at $x = 0.05$.

The anomalous component of $\alpha(T)$ in the cubic phase of all the compositions exists at nearly the same temperature $T_d \approx 430$–450 K, which correlates to the behavior of the permittivity.

5. DISCUSSION

The phase diagram of the $Ba_{1-x}Bi_{2x/3}TiO_3$ system is depicted in Fig. 3, where, along with the data obtained from the thermal expansion, the results of studying the dielectric properties and also the data from [11] are presented. In the concentration range under study, the quantities T_c, T_1, T_2, and T'_m well agree within the limits of the error of their determination.

As noted in Section 1, the phase diagrams of the solid solutions based on substitution of trivalent lanthanum and trivalent bismuth are substantially different. This circumstance can be due to a difference in

the mechanisms of charge compensation [8, 11, 14, 15].

As bismuth is added, the compensation is realized at the expense of the formation barium vacancies, which leads to the compound formula $Ba_{1-x}\square_{x/3}Bi_{2x/3}TiO_3$ [6]. Upon substitution of lanthanum for barium, the charge compensation occurs as a result of the formation of titanium vacancies (the compound formula is $Ba_{1-x}La_xTi_{1-x/4}\square_{x/4}O_3$) [8, 15]. In the latter case, the doping leads to changes in the ferroelectrically active positions B in the perovskite lattice and, thus, to substantial change in the temperatures of the ferroelectric phase transitions, as is the case in the $BaTi_{1-x}M_xO_3$ (M = Zr, Sn, ...) [5, 6].

In [14], the spectra of vibrational frequencies and temperatures of instability of the cubic lattice in solid solutions $Ba_{1-x}\square_{x/3}Bi_{2x/3}Ti(Zr)O_3$ and $Ba_{1-x}La_xTi(Zr)_{1-x/4}\square_{x/4}O_3$ were calculated in the framework of the generalized Gordon–Kim model with allowance for dipole and quadrupole polarizabilities of ions. It was shown that the character of the ferroelectric instability is more likely determined by the position of vacancy formation and ion type in the oxygen octahedron center than by the type of impurity. In the solid solutions with the heavy zirconium ion, the ferroelectricity is mainly due to the motion of ions occupying the barium position and the oxygen in the direction perpendicular to the Zr–O bond. In the solid solutions containing lighter titanium, the ferroelectric instability is due to the motion of another pair of titanium and oxygen ions along the Ti–O bond. The calculated dependences of the temperature T_c on the Bi^{3+} concentration qualitatively agree with the experimental data. In the case of doping with La^{3+}, the agreement exists, assuming that as the lanthanum concentration increases, the vacancies form in both the Ti^{4+} positions and (at $x > 0.1$) the Ba^{2+} positions.

Unfortunately, in [14], no transitions between distorted phases were considered. However, as the dopant is bismuth, most substantial changes in the properties of the solid solutions occur at temperatures lower than T_c. The bismuth doping quickly (at $x > 0.02$) brings about the wedging-out the $C2mm$ phase and occurrence very unusual relaxor phenomena at T_m inside the ferroelectric state, according to [11].

To describe the phase transitions in barium titanate and other ferroelectrics, along with the microscopic models and ab initio calculations, an approach based on the Landau phenomenological theory is also developed. Such an approach was successfully used to describe the permittivity, polarization, deformation, and T–E phase diagrams of $BaTiO_3$ [16–18]. In $BaTiO_3$, the order parameter is the spontaneous polarization $P = (P_1, P_2, P_3)$, and the thermodynamic potential was written in [17, 18] as the polynomial to the eight power in components P_i ($i = 1, 2, 3$)

$$\begin{aligned}\Delta G = {} & a_1(P_1^2 + P_2^2 + P_3^2) + a_{11}(P_1^4 + P_2^4 + P_3^4) \\ & + a_{12}(P_1^2P_2^2 + P_2^2P_3^2 + P_1^2P_3^2) + a_{111}(P_1^6 + P_2^6 + P_3^6) \\ & + a_{112}[P_1^2(P_2^4 + P_3^4) + P_2^2(P_1^4 + P_3^4) + P_3^2(P_1^4 + P_2^4)] \\ & + a_{123}P_1^2P_2^2P_3^2 + a_{1111}(P_1^8 + P_2^8 + P_3^8) \\ & + a_{1112}[P_1^6(P_2^2 + P_3^2) + P_2^6(P_1^2 + P_3^2) + P_3^6(P_1^2 + P_2^2)] \\ & + a_{1122}(P_1^4P_2^4 + P_2^4P_3^4 + P_1^4P_3^4) \\ & + a_{1123}(P_1^4P_2^2P_3^2 + P_2^4P_3^2P_1^2 + P_3^4P_1^2P_2^2) \\ & - E_1P_1 - E_2P_2 - E_3P_3 + \ldots,\end{aligned} \tag{1}$$

where the coefficient a_1 is linearly dependent on temperature, and it obeys the Curie–Weiss law, and the spontaneous strain is determined by relationships

$$\begin{aligned} e_{11} &= Q_{11}P_1^2 + Q_{12}P_2^2 + Q_{12}P_3^2, \\ e_{22} &= Q_{12}P_1^2 + Q_{11}P_2^2 + Q_{12}P_3^2, \\ e_{33} &= Q_{12}P_1^2 + Q_{12}P_2^2 + Q_{11}P_3^2. \end{aligned} \tag{2}$$

In $BaTiO_3$, the strain is mainly determined by the square of the spontaneous macroscopic polarization and, thus, can be used for its estimation.

$$\frac{\Delta L}{L} = \int \alpha_L(T)dT + (Q_{11} + 3Q_{12})P^2. \tag{3}$$

Here, $\alpha_L(T)$ is the lattice thermal expansion coefficient (no anomalous); Q_{11} and Q_{12} are the electrostriction coefficients.

To select the anomalous contribution to the strain $(Q_{11} + Q_{12})P^2$ and to find the polarization P, it is necessary to adequately describe nonanomalous contribution to the strain and the thermal expansion coefficient $\alpha_L(T)$.

The traditional approach [19–21] in which the elongation $\Delta L/L(T)$ is approximated, at high temperatures, by a linear dependence does not adequately describe the experimental data with distance from T_c to a low-temperature range, since the $\Delta L/L(T)$ temperature dependence is clearly nonlinear, and the thermal expansion coefficient $\alpha(T)$ is not constant. Thus-determined values of the anomalous contributions to the deformation and the root-mean-square polarization are, as a rule, overestimated, and they are dependent on the temperature range in which the approximation is performed [9, 13]. According to the theory of thermal expansion, the coefficient α above the Debye temperature is even if slightly dependent on temperature, which leads to a nonlinearity of the deformation. In addition, at high temperatures, there

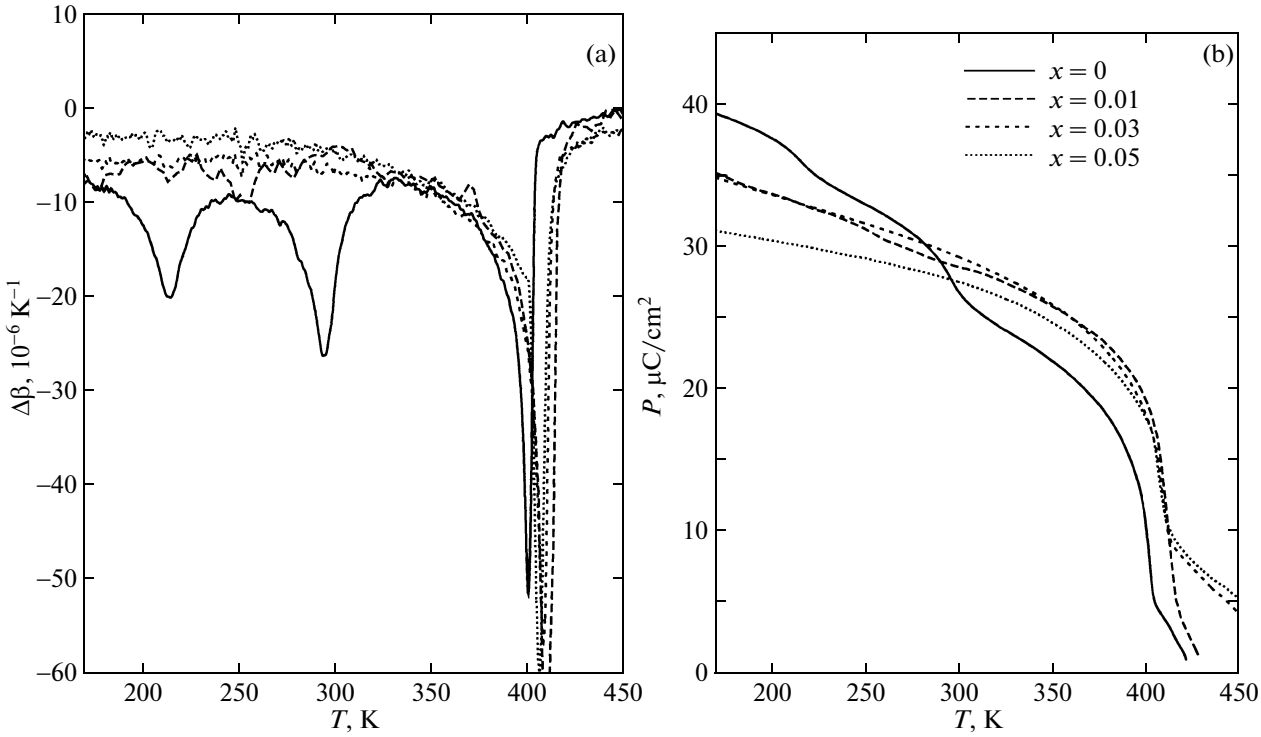

Fig. 4. Temperature dependences of (a) the anomalous component of the thermal expansion coefficient β and (b) the polarization of the solid solutions $Ba_{1-x}Bi_{2x/3}TiO_3$.

are additional contributions to the deformation due to thermostimulated defects, and this fact is also demonstrated by the high-temperature behavior of the thermal expansion coefficient $\alpha(T)$. As temperature decreases, the thermal expansion coefficient must tend to a zero, and, to estimate the polarization at low temperatures ($T < T_c^2 < \Theta_D$), it is necessary to take into account the relation between the thermal expansion and the heat capacity and its temperature dependence, if only in terms of the Debye model. Since, in the cubic phase ($T > T_c \approx \Theta_D$), the thermal expansion coefficient is slightly dependent on temperature, and it is impossible to determine the Debye temperature from an approximation of the experimental data, we use the average value $\Theta_D \approx 432$ K [22]. The data on the temperature dependence of the volume thermal expansion coefficient $\beta(T) = 3\alpha(T)$ were processed using the relationship

$$\beta(T) = aT + bC_D(T), \tag{4}$$

where a and b are the adjustable parameters.

$$C_D(x) = 9R\left(\frac{\Theta_D}{T}\right)^3 \int_0^{\Theta_D/T} t^4 \frac{\exp(t)}{(\exp(t)-1)^2} dt = 3R\left[4D_3(x_D) - \frac{3x_D}{\exp(x_D)-1}\right], \tag{5}$$

where $x_D = \Theta_D/T$, and $D_3(x_D)$ is the third-order Debye function.

Figure 4a shows the anomalous components of the thermal expansion coefficient β obtained as a result of processing of the experimental data in terms Eq. (4).

The temperature dependences of the polarization calculated from the deformation of the ceramic samples are shown in Fig. 4b. The polarization was calculated, assuming that the electrostriction coefficients Q_{11} and Q_{12} [23, 24] are independent of temperature. For the solid solutions $Ba_{1-x}Bi_{2x/3}TiO_3$, we used the same values of the electrostriction coefficients that were used for pure $BaTiO_3$.

As the bismuth concentration increases, the polarization increases near T_c in the tetragonal phase with all the concentrations, and it decreases in the orthorhombic and rhombohedral phases as compared to pure $BaTiO_3$.

In [16, 17], based on an analysis of the thermodynamic potential, the T–E phase diagrams of barium titanate were calculated as an external electric field was applied along the [100], [101], and [111] directions. These phase diagrams are similar, in some sense, to the temperature–impurity concentration phase diagrams for the solid solutions. In particular, at certain strengths and direction of the electric field, the wedging-out of intermediate distorted phases is possible.

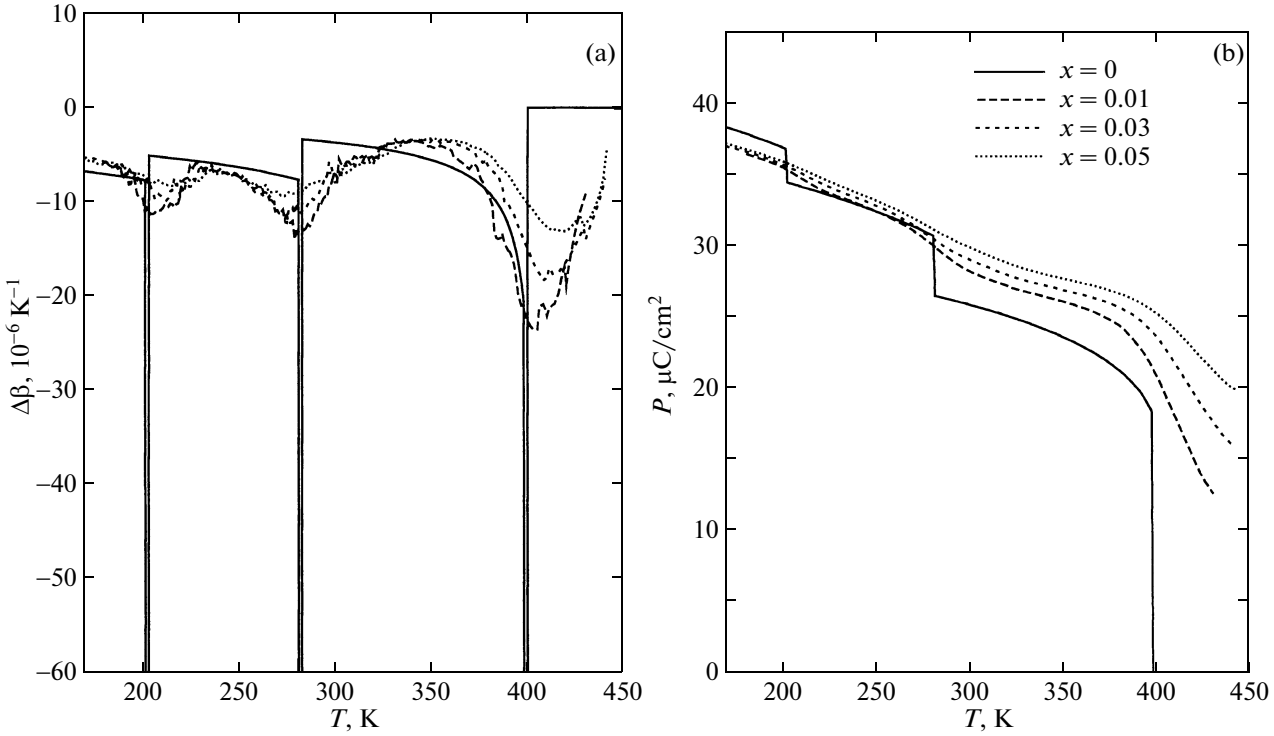

Fig. 5. Calculated temperature dependences of (a) the anomalous component of the thermal expansion coefficient β and (b) the polarization of the solid solutions $Ba_{1-x}Bi_{2x/3}TiO_3$.

It may be suggested that charged defects (Bi^{3+} ions and vacancies in Ti^{4+}) induce random electric fields in the crystal lattice; the fields increases with the concentration and lead to the formation of heterogeneous ferroelectric states and wedging-out of intermediate phases.

We calculated the distributions of random electric fields at the sites of the crystal lattice consisting of $20 \times 20 \times 20$ cells at various Bi concentrations in terms of the simple electrostatic model of randomly distributed point defects. Using these distributions and the thermodynamic potential (1) with allowance for random electric fields, we calculated the temperature dependences of the rms polarization and the anomalous component of the volume thermal expansion coefficient (Fig. 5).

As seen from the comparison of Fig. 5 with Fig. 4, there is only qualitative agreement between the calculated and experimental $\Delta\beta(T)$ and $P(T)$ dependences and the character of the concentration dependences of temperatures of the anomalies. The temperature T_c increases, but the anomalies at T_1 and T_2 are strongly smeared and approach one other as the bismuth concentration increases. We failed to obtain a wedging-out of the intermediate phase. This fact is most likely due to the simple model that does not take into account the interaction between local distortions.

6. CONCLUSIONS

Thus, the studies performed revealed the anomalous behavior of the deformation and the thermal expansion coefficient of ceramic $Ba_{1-x}Bi_{2x/3}TiO_3$ materials, and the T–x phase diagram was refined. From the data on the thermal expansion, we found the temperature dependences of the root-mean-square polarization.

ACKNOWLEDGMENTS

This study was supported by the Council on Grants from the President of the Russian Federation for the Support of Leading Scientific Schools (grant NSh-4645.2010.2).

REFERENCES

1. D. Hennings, A. Schnell, and G. Simon, J. Am. Ceram. Soc. **65**, 539 (1982).
2. J. Ravez and A. Simon, Eur. J. Solid State Inorg. Chem. **34**, 1119 (1997)
3. R. Farhi, M. El. Marssi, A. Simon, and J. Ravez, Eur. Phys. J. B **9**, 599 (1999).
4. J. Ravez and A. Simon, Phys. Status Solidi A **178**, 793 (2000).
5. C. Ang, Z. Jing, and Z. Yu, J. Mater. Sci. **38**, 1057 (2003).

6. A. Simon, J. Ravez, and M. Maglione, J. Phys.: Condens. Matter **16**, 963 (2004).
7. M. Kchikech and M. Maglione, J. Phys.: Condens. Matter **6**, 10159 (1994).
8. F. D. Morrison, D. C. Sinclair, and A. R. West, J. Appl. Phys. **86**, 6355 (1999).
9. M. Gorev, V. Bondarev, I. Flerov, M. Maglione, A. Simon, Ph. Sciau, M. Boulos, and S. Guillement-Fritsch, J. Phys.: Condens. Matter **21**, 075902 (2009).
10. F. Bahri, A. Simo, H. Khemakhem, and J. Ravez, Phys. Status Solidi A **184**, 459 (2001).
11. A. Simon, J. Ravez, and M. Maglione, Solid State Sci. **7**, 925 (2005).
12. V. Mueller, L. Jager, H. Beige, H.-P. Abicht, and T. Muller, Solid State Commun. **129**, 757 (2004).
13. Y. He, Thermochim. Acta **419**, 135 (2004).
14. N. G. Zamkova and V. I. Zinenko, Phys. Solid State **51** (5), 973 (2009).
15. F. D. Morrison, A. M. Coats, D. C. Sinclair, and A. R. West, J. Electroceram. **6**, 219 (2001).
16. A. J. Bell, J. Appl. Phys. **89**, 3907 (2001).
17. Y. L. Li, L. E. Cross, and L. Q. Chen, J. Appl. Phys. **98**, 064101 (2005).
18. Y. L. Wang, A. K. Tagantsev, D. Damjanovic, N. Setter, V. K. Yarmarkin, A. I. Sokolov, and I. A. Lukyanchuk, J. Appl. Phys. **101**, 104515 (2007).
19. G. Burns and F. H. Dacol, Phys. Rev. B: Condens. Matter **28**, 2527 (1983).
20. A. S. Bhalla, R. Guo, L. E. Cross, G. Burns, F. H. Dacol, and R. R. Neurgaonkar, Phys. Rev. B: Condens. Matter **36**, 2030 (1987).
21. S. Wingsaenmai, R. Yimnirum, S. Ananta, R. Guo, and A. S. Bhalla, Mater. Lett. **62**, 352 (2008).
22. W. N. Lawless, Phys. Rev. B: Solid State **17**, 1458 (1978).
23. G. A. Smolenskii, V. A. Bokov, V. A. Isupov, N. N. Krainik, R. E. Pasynkov, and M. S. Shur, *Ferroelectrics and Antiferroelectrics* (Nauka, Leningrad, 1971) [in Russian].
24. S. Nomura and K. Uchino, Ferroelectrics **41**, 117 (1982).

Translated by Yu. Ryzhkov